Comparison of different *in vitro* cell models for the assessment of pesticide-induced dopaminergic neurotoxicity

Harm J. Heusinkveld, Remco H.S. Westerink*

Neurotoxicology Research Group, Division of Toxicology, Institute for Risk Assessment Sciences (IRAS), Faculty of Veterinary Medicine, Utrecht University, P.O. Box 80. 177, NL-3508 TD Utrecht, The Netherlands

A R T I C L E   I N F O

A B S T R A C T

Biomedical and (neuro) toxicity research on (neuro) degenerative diseases still relies strongly on animal models. However, the use of laboratory animals is often undesirable for both ethical and technical reasons. Current *in vitro* research thus largely relies on tumor derived- or immortalized cell lines. Notably, the suitability of cell lines for studying neurodegeneration is determined by their intrinsic properties. We therefore characterized PC12, SH-SY5Y, MES23.5 and N27 cells with respect to the presence of functional membrane ion channels and receptors as well as for the effects of five known neurotoxic pesticides on cytotoxicity, oxidative stress and parameters of intracellular calcium homeostasis using a combined alamar Blue/CFDA assay, a H_2DCFDA assay and single cell fluorescent (Fura-2) calcium imaging, respectively. Although all pesticides demonstrated a certain level of functional neurotoxicity in the different cell lines, our results also demonstrate considerable differences in intrinsic properties and pesticide-induced effects between the cell lines.

This clearly indicates that care should be taken when interpreting (neuro)toxicity data as the chosen cell model may greatly influence the outcome.

1. Introduction

Current (neuro) toxicity and biomedical research on human (degenerative) diseases of the nervous system relies strongly on animal models, mainly rodents. According to the 2010 EU report on the annual laboratory animal use (SEC2010/1107) biomedical- and toxicological research involved nearly 2.5 million animals. These animal experiments are not only ethically debated but also expensive, time-consuming and unsuitable for high-throughput testing. *In vitro* approaches, in contrast, provide a relatively fast and cheap way of testing chemicals for their (neuro) toxic properties without the need for the extensive use of laboratory animals (Westerink, 2013).

Available *in vitro* techniques to study pathways of neurotoxicity and neurodegeneration rely mainly on chemical-induced effects in a wide array of (often tumor-derived, rodent or human) cell lines or pluripotent (embryonic, rodent or human) stem cells. Although stem cells provide the unique opportunity to study (developmental) neurotoxicity in a complex network, homogeneous cell lines allow for in-detail, single-cell studies dissecting (human relevant) molecular pathways. Therefore, toxicological research on potential neurotoxic properties of compounds could focus on *in vitro* strategies using one or more cell lines from the wide array of cell lines available.

Various cell models are reported to have dopaminergic properties and should thus be suitable for *in vitro* studies on dopaminergic neurotoxicity, which could aid in studying for example Parkinson's Disease (PD). However, the suitability of a cell model for answering a particular research question relies largely on its intrinsic (functional) properties. Hence, it is striking that many cell lines are poorly characterized with respect to intrinsic properties, including the presence of important membrane receptors and ion channels.

As neurotoxicity of a compound is often determined by the presence of a particular transporter (*e.g.* dopaminergic toxicity of MPP^+ *via* uptake by dopamine membrane transporters (DAT)) or membrane receptor (*e.g.* excitotoxicity by activation of glutamatergic neurotransmitter receptors), the use of an inappropriate model may lead to an erroneous estimation of (neuro) toxicity. We therefore chose to characterize four catecholaminergic cell lines (rat PC12, human SH-SY5Y, mouse/rat hybrid MES23.5 and rat N27 cells) with respect to functional properties.

Rat pheochromocytoma cells (**PC12**; (Greene and Tischler, 1976) provide a widely used model in neurotoxicology that has been extensively characterized for neurosecretion and the presence of ion channels and neurotransmitter receptors (Shafer and Atchison, 1991; Westerink and Ewing, 2008). Although these cells originate from an

---

Table 1

Dopaminergic properties of the different catecholaminergic cell lines.

	VGCC*	TH	DA	DAT	VMAT	Vesicular release
PC12	L,N,P/Q-type[1,13]	+[6,7]	+[6,7]	+[6,7]	+[6,7]	+[7,12]
MES23.5	N-type[2,8,10]	+[2]	+[2]	+[2]	Unk.	Unk.
SH-SY5Y	L, N-type[3,9,14,16,17]	+[3,11]	+[3,11]	+[3,11]	+[3,11]	+[15,16]
N27	Unk.	+[4,5]	Unk	+[4,5]	Unk.	Unk.

VGCC: voltage-gated calcium channels; TH: tyrosine hydroxylase; DA: dopamine; DAT: dopamine transporter; VMAT: vesicular monoamine transporter; + = present; Unk.: unknown; *Functional voltage-gated calcium channels: L type: Ca_v1, dihydropyridine-sensitive; N-type Ca_v 2.2, ω-Conotoxin GVIA sensitive; P/Q type: $Ca_v2.1$, ω-Conotoxin MVIIC sensitive.

[1] Dingemans et al., 2009; [2] Crawford et al., 1992; [3] Biedler et al., 1973; [4] Prasad et al., 1994; [5] Adams et al., 1996; [6] Shafer and Atchison, 1991; [7] Westerink and Ewing, 2008; [8] Gleeson et al., 2015; [9] Sousa et al., 2013; [10] Schneider et al., 1995; [11] Chen et al., 2013; [12] Tully and Treistman, 2004; [13] Lerner et al., 2006; [14] Zhu et al., 2016; [15] Zhao et al., 2012; [16] Vaughan et al., 1995; [17] Reuveny and Narahashi, 1993.

(non-neuronal) adrenal tumor, they display several characteristics of mature dopaminergic neurons (Table 1). This renders the PC12 cell a suitable model for the study of catecholaminergic neurotoxicity *in vitro* (Heusinkveld et al., 2016; Meijer et al., 2014).

The **SH-SY5Y** cell line (Biedler et al., 1973) is a catecholaminergic neuroblastoma cell line from human origin, widely used to study neurotoxicity *in vitro* (Faria et al., 2016; Sala et al., 2016). SH-SY5Y cells synthesize and release noradrenaline (Table 1) through vesicular release (*i.e.*, exocytosis) (Vaughan et al., 1995; Zhao et al., 2012). The hybrid **MES23.5** cell line is a product of somatic fusion of rat embryonic mesencephalon cells and the murine N18TG2 neuroblastoma-glioma cell line (Crawford et al., 1992). The resulting hybrid cell line displays many characteristics of mesencephalic dopaminergic neurons (Table 1). The **N27** cell line is an immortalized cell line derived from TH-positive fetal rat mesencephalic neurons (Prasad et al., 1994; Table 1). These cells are increasingly used to study *in vitro* (parkinsonian) dopaminergic neurodegeneration (see *e.g.* Song et al., 2011; Xu et al., 2016).

As pesticides are implicated in *in vivo* and *in vitro* neurotoxicity, a reference set of five pesticides was composed consisting of rotenone, lindane, dieldrin, imazalil and dinoseb. These pesticides all display, to a certain extent, dopaminergic neurotoxicity albeit with a different mechanism of action. Rotenone is a well-known model compound for inducing PD *via* mitochondrial uncoupling (complex I) *in vivo* and is therefore extensively used to study dopaminergic neurodegeneration, both *in vivo* and *in vitro* (see *e.g.* Dawson and Dawson, 2003; Greenamyre et al., 2010). The dinitrophenolic herbicide dinoseb is also a mitochondrial uncoupler (complex III; Palmeira et al., 1994), that has recently also been linked to Ca^{2+}-mediated activation of pathways implicated in dopaminergic neurodegeneration *in vitro* (Heusinkveld et al., 2016).

The organochlorine insecticides lindane and dieldrin are classical neurotoxicants *in vitro* as well as *in vivo* and are implicated in the etiology of PD (Corrigan et al., 2000; Franco et al., 2010). The primary mechanism underlying lindane and dieldrin-induced neurotoxicity is inhibition of GABA receptors (Anand et al., 1998; Vale et al., 2003). In addition, both lindane and dieldrin have been linked to disturbance of intracellular calcium homeostasis (Heusinkveld and Westerink, 2012). Furthermore, the azole fungicide imazalil has been linked to adverse neurobehavioural effects *in vivo* (Tanaka, 1995) and was recently linked to disturbance of the intracellular calcium homeostasis (Heusinkveld et al., 2013).

Intracellular Ca^{2+} homeostasis plays a pivotal role in neuronal function, development and survival of dopaminergic cells (Gleichmann and Mattson, 2011). Therefore, we characterized the four cell lines with regards to functional parameters, such as the presence of functional neurotransmitter receptors and ion channels. Furthermore, effects of the reference pesticides on basal- and depolarization-evoked changes in the intracellular Ca^{2+} concentration ($[Ca^{2+}]_i$) were investigated. As cell death and oxidative stress are clearly implicated in neurotoxicity

and degeneration (Goodwin et al., 2013), the effects on cell viability and production of reactive oxygen species (ROS) upon exposure to the reference set of pesticides were also assessed in all cell lines.

2. Materials & methods

2.1. Chemicals

Fura-2 AM, CFDA-AM and 2,7-dichlorodihydrofluorescein diacetate (H_2DCFDA) were obtained from Molecular Probes (Invitrogen, Breda, The Netherlands). Unless otherwise noted, all other chemicals including neurotransmitters were obtained from Sigma (Zwijndrecht, The Netherlands). The pesticides used as reference compounds (lindane, dieldrin, imazalil, dinoseb and rotenone) were obtained Pestanal® grade, 99.8% purity (Riedel de Haën, Seelze, Germany). Saline solutions, containing (in mM) 125 NaCl, 5.5 KCl, 2 $CaCl_2$, 0.8 $MgCl_2$, 10 HEPES, 24 glucose and 36.5 sucrose (pH 7.3, adjusted using HCl), were prepared with de-ionized water (Milli-Q®; resistivity > 18 MΩ·cm). Stock solutions of 0.1–100 mM pesticide were prepared in DMSO and diluted in saline (Ca^{2+} imaging) or serum-free medium (cell viability and ROS production) just prior to the experiments. All solutions used in experiments, including control experiments, contained 0.1% DMSO.

2.2. Cell culture

PC12 cells (Greene and Tischler, 1976) were grown in RPMI 1640 (Invitrogen, Breda, The Netherlands) supplemented with 5% fetal calf serum (FCS) and 10% horse serum (HS; ICN Biomedicals, Zoetermeer, The Netherlands). MES23.5 hybridoma cells (kindly provided by Dr. S. Appel (Methodist Neurological Institute, Houston TX, USA)) were grown in DMEM (Invitrogen, Breda, The Netherlands) supplemented with 10% FCS, 2% HEPES and Satos supplements (Crawford et al., 1992). Human SH-SY5Y cells (kindly provided by Dr. R. van Kesteren (VUmc, Amsterdam, The Netherlands)) were grown in 50/50 DMEM/F-12 medium (Invitrogen, Breda, The Netherlands) supplemented with 15% FCS. Rat N27 cells (kindly provided by Dr. JM Fuentes (Univ. de Extremadura, Caceres, Spain)) were cultured in RPMI 1640 supplemented with FCS (10%). All cells were grown for no more than 8 passages to avoid the possible influence of senescence. All cells were grown in a humidified incubator at 37 °C and 5% CO_2.

All cell culture materials were either poly-L-lysine coated (PC12 & MES23.5) or uncoated (SH-SY5Y and N27). For cell viability experiments, cells were sub-cultured in 24-wells plates (Greiner Bio-one, Solingen, Germany) at a (near confluency) density of 5×10^5 (PC12) or 2×10^5 cells/well (MES23.5, SH-SY5Y and N27). For experiments assessing production of ROS, cells were sub-cultured in 48-wells plates (Greiner Bio-one, Solingen, Germany) at a (near confluency) density of 2.5×10^5 (PC12) or 5×10^4 (MES23.5, SH-SY5Y and N27) cells/well. For Ca^{2+} imaging experiments, cells were sub-cultured in poly-L-lysine coated (PC12 & MES23.5) or uncoated (SH-SY5Y and N27) 35 mm glass-bottom dishes (glass surface 78mm^2) (MatTek, Ashland, MA) at a density of $1–1.5 \times 10^6$ cells/dish.

2.3. Ca^{2+} imaging

Changes in $[Ca^{2+}]_i$ were measured on a single-cell level using the Ca^{2+}-sensitive fluorescent ratio dye Fura-2 AM as described previously (Heusinkveld et al., 2013). Briefly, cells were loaded with 5 μM Fura-2 AM (Molecular Probes; Invitrogen, Breda, The Netherlands) for 20 min at room temperature, followed by 15 min de-esterification. After de-esterification, the cells were placed on the stage of an Axiovert 35M inverted microscope (Zeiss, Göttingen, Germany) equipped with a TILL Photonics Polychrome IV (TILL Photonics GmbH, Gräfelfing, Germany). Fluorescence, evoked by 340 and 380 nm excitation wavelengths (F340 and F380), was collected every 6 s at 510 nm with an Image SensiCam digital camera (TILL Photonics GmbH).

To characterize the presence of functional neurotransmitter receptors and ion channels, cells were exposed to K^+ (KCl; 100 mM), serotonin (serotonin hydrochloride; 5-HT; 100 μM) acetylcholine (acetylcholine chloride; ACh; 100 μM), glutamate (monosodium glutamate; 100 μM) or ATP (Adenosine 5′-triphosphate disodium salt hydrate; 100 μM) following a 5 min baseline recording.

To investigate compound-induced effects on basal and depolarization-evoked $[Ca^{2+}]_i$, cells were depolarized by high-K^+ containing saline (100 mM K^+) for 18 s after a 5 min baseline recording. This provides a robust depolarization to ~0 mV depending on the resting potential of the cell. This depolarization is sufficient to open both high- and low voltage-activated VGCCs. Following a 10 min recovery period, cells were exposed to DMSO (0.1%), or one of the reference compounds for 20 min (indicated by the dashed line in Fig. 2A) to evaluate the effects on basal $[Ca^{2+}]_i$. Subsequently, cells were depolarized for a second time to evaluate effects of exposure on depolarization-evoked Ca^{2+}-influx. This is calculated as the treatment ratio (TR; %) between the first and second depolarization-evoked $[Ca^{2+}]_i$ peak values relative to control.

2.4. Cell viability assays

To assess the effects of the compounds on cell viability a combined alamar Blue/CFDA-AM (aB/CFDA) assay was used (protocol adapted from Bopp and Lettieri, 2008) to determine respectively mitochondrial activity and membrane integrity. Cells were exposed in serum- and phenol red-free medium to concentrations up to 100 μM for up to 24 h. Mitochondrial activity of the cells was recorded as a measure of cell viability with the aB assay, which is based on the ability of the cells to reduce resazurin to resorufin. In the same experiment, membrane integrity was assessed indirectly using a CFDA-AM assay, which is based on non-specific cytoplasmic-esterase activity. Briefly, cells were incubated for 30 min with 12,5 μM aB and 4 μM CFDA-AM. Resorufin was measured spectrophotometrically at 540/590 nm (Infinite M200 microplate; Tecan Trading AG, Männedorf, Switzerland), whereas hydrolysed CFDA was measured spectrophotometrically at 493/541 nm.

2.5. Production of ROS

The involvement of oxidative stress in the observed reduction in cell viability was investigated using the fluorescent dye H_2DCFDA as described previously (Heusinkveld et al., 2010). Briefly, cells were loaded with 1.5 μM H_2DCFDA for 30 min at 37 °C. Subsequently, cells were exposed for up to 24 h to 0.1–100 μM compound and fluorescence was measured spectrophotometrically at 488/520 nm (Infinite M200 microplate; Tecan Trading AG, Männedorf, Switzerland).

2.6. Data-analysis and statistics

Data from cell viability and ROS experiments were generated in at least 3 individual experiments ($N \geq 3$) consisting of at least 3 replicates per experiment ($n \geq 9$). Cell viability data (aB/CFDA) are presented as % viability ± standard error of the mean (SEM; calculated using the N) compared to DMSO controls. Data on production of ROS are presented as % increase in ROS ± SEM (calculated using the N) compared to time-matched DMSO controls. A relevant effect size in cell viability and ROS experiments, indicated as lowest observed effect concentration (LOEC), is defined as the concentration that induces a ≥ 20% change in the parameter assessed.

Data from single-cell fluorescence microscopy is presented as F340/F380 ratio (R), reflecting changes in $[Ca^{2+}]_i$, and analyzed using custom-made MS-Excel macros applying a correction for background fluorescence (Heusinkveld et al., 2013). The data represent average values derived from 15 to 63 individual cells (n) in 3–6 independent experiments (N).

Statistical analyses were performed using GraphPad Prism v6.01 (GraphPad Software, San Diego, California, USA). Concentration-response curves were fitted for experiments assessing cell viability and ROS production using a nonlinear sigmoidal or bell-shaped curve-fit when applicable.

3. Results

3.1. Characterization of neurotransmitter receptors and ion channels

To characterize the different cell lines with respect to the presence of functional Ca^{2+}-permeable receptors and ion channels, cell lines were stimulated with different stimuli and $[Ca^{2+}]_i$ was monitored using single-cell fluorescence microscopy.

Upon depolarization with 100 mM K^+, an increase in $[Ca^{2+}]_i$ was observed in PC12, SH-SY5Y and MES23.5 cells, indicative of the presence of VGCCs. The largest increase in $[Ca^{2+}]_i$ was observed in PC12 cells, followed by MES23.5 and SH-SY5Y cells. N27 cells displayed no increase in $[Ca^{2+}]_i$ upon depolarization. Similarly, upon stimulation with 100 μM ACh, an increase in $[Ca^{2+}]_i$ was observed in PC12, MES23.5 and SH-SY5Y cells, suggestive for the presence of ionotropic and/or metabotropic ACh receptors. However, no response was detected in N27 cells. PC12, MES23.5 and N27 responded to stimulation with 100 μM ATP, indicative of the presence of purinergic receptors. However, SH-SY5Y did not respond to ATP. When stimulated with 100 μM serotonin (5-HT) only the MES23.5 cells responded with an increase in $[Ca^{2+}]_i$, whereas the other cell lines showed no change in $[Ca^{2+}]_i$. None of the cell lines responded to stimulation with glutamate (100 μM), neither with nor without prior depolarization with 100 mM K^+, suggestive for the absence of functional ionotropic glutamate receptors.

3.2. Pesticide-induced changes in $[Ca^{2+}]_i$

The concentrations of the pesticides applied to assess the effects on the $[Ca^{2+}]_i$ were chosen based on pilot experiments or previous results in which they were proven effective in PC12 cells without overt acute cytotoxicity.

In PC12, SH-SY5Y and MES23.5 cells, depolarization with 100 mM K^+ resulted in a fast, transient increase in $[Ca^{2+}]_i$ due to opening of VGCCs. $[Ca^{2+}]_i$ rapidly recovered to near-baseline values. Repeated depolarization in control cells resulted in treatment ratios (TR) of ~90 ± 16% (n = 80), 65 ± 21% (n = 29) and 90 ± 29% (n = 53) for respectively PC12, SH-SY5Y and MES23.5 cells. As the characterization experiments (Fig. 1) revealed the absence of functional VGCCs in N27 cells, effects on depolarization-evoked Ca^{2+}-influx could not be tested in N27 cells.

3.3. Basal Ca^{2+}

Upon exposure to lindane (100 μM), a transient increase in basal $[Ca^{2+}]_i$ was observed in PC12 cells (Fig. 2A) in line with earlier measurements (Heusinkveld et al., 2010), whereas no change in basal $[Ca^{2+}]_i$ was observed in SH-SY5Y, MES 23.5 or N27 cells (Fig. 2B). Following exposure to dinoseb (30 μM) an increase in basal $[Ca^{2+}]_i$ was observed in all cell lines although the nature of the increase in PC12, MES23.5 and N27 was transient, whereas in SH-SY5Y cells a transient increase was followed by a sustained elevated level of basal $[Ca^{2+}]_i$. No change in basal $[Ca^{2+}]_i$ was observed upon exposure to dieldrin (10 μM), rotenone (10 μM) or imazalil (30 μM) in any of the cell lines (Fig. 2).

3.4. Depolarization-evoked Ca^{2+}

Exposure to lindane (100 μM), dieldrin (10 μM), imazalil (30 μM) and rotenone (10 μM) induced a comparable decrease in depolarization-evoked $[Ca^{2+}]_i$ in PC12, SH-SY5Y and MES23.5 cells (Fig. 2).
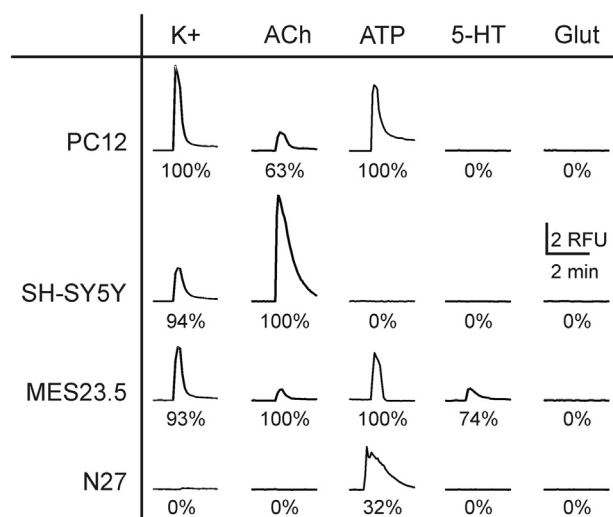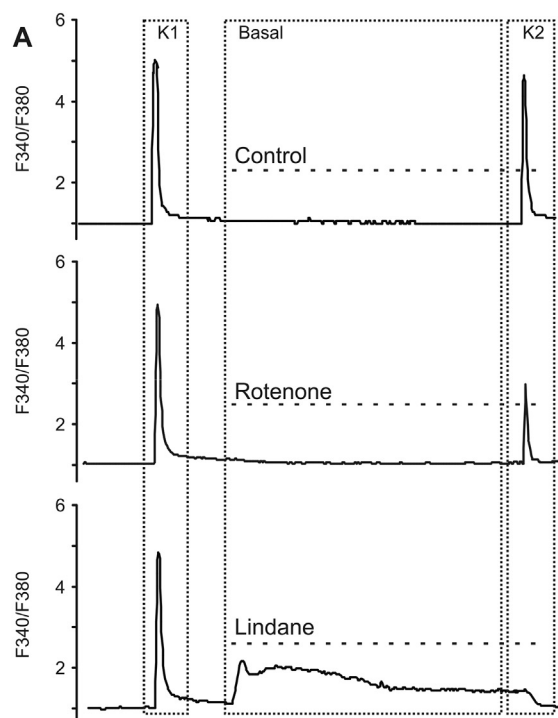
Fig. 1. Average traces of the increase in $[Ca^{2+}]_i$ observed in the cell lines upon exposure to different stimuli. Percentages indicated below the traces represent the fraction of cells that responded to the particular stimulus (3–6 independent experiments; 15–63 individual cells).

Although the extent to which the depolarization-evoked increase in $[Ca^{2+}]_i$ was inhibited by dieldrin and rotenone was comparable in all three cell lines, differential levels of inhibition were observed for imazalil (PC12 = MES23.5 > SH-SY5Y) and lindane (PC12 > SH-SY5Y > MES23.5). Dinoseb did not change the depolarization-evoked increase in $[Ca^{2+}]_i$ in PC12 cells (TR: 105 ± 38%, n = 40), whereas in MES23.5 the depolarization-evoked increase in $[Ca^{2+}]_i$ was increased (TR: 129 ± 66%, n = 36, p ≤ 0.01), and in SH-SY5Y it was inhibited (TR: 29 ± 14%, n = 35, p ≤ 0.001).

3.5. Membrane integrity, mitochondrial activity and ROS production

To assess differences between cellular responses to pesticide exposure (0.1–100 μM; 24 h), mitochondrial activity and membrane integrity were assessed using a combined alamar Blue (aB) and CFDA assay. To assess the involvement of ROS production in the observed changes in cell viability, cumulative ROS production was measured using the fluorescent dye H_2DCFDA.

Exposure to lindane did not result in changes in mitochondrial activity in the different cell lines (Fig. 3A1). Solely in the MES23.5 cells a small decrease in membrane integrity was observed at the highest concentration (100 μM; Fig. 3B1). No increase in ROS production was observed in any of the cell lines upon exposure to lindane (Fig. 3C1). Exposure to dieldrin resulted in all cell lines in an increase in mitochondrial activity (LOEC PC12 and SH-SY5Y 10 μM; LOEC N27 and MES23.5 0.1 μM). In N27 and MES23.5 cells, the increase in mitochondrial activity was followed by a decrease in activity at higher concentrations (> 10 μM) (Fig. 3A2). Membrane integrity was affected solely in MES23.5 cells (LOEC: 10 μM; Fig. 3B2). No increase in ROS production was observed in any of the cell lines upon exposure to dieldrin (Fig. 3C2). Exposure to imazalil resulted in an increase in mitochondrial activity in all cell lines (LOECs PC12: 1 μM; SH-SY5Y: 10 μM; MES23.5: 100 μM; N27: 10 μM; Fig. 3A3). In PC12, MES23.5 and N27 cells the increase in mitochondrial activity was paralleled by a decrease in membrane integrity (all three LOEC: 100 μM; Fig. 3B3). No change in membrane integrity was observed in SH-SY5Y cells. Exposure to imazalil did induce ROS production, but solely in PC12 cells (LOEC: 100 μM; Fig. 3C3). Exposure to dinoseb resulted in a bi-phasic change in mitochondrial activity in both PC12 and N27 cells (LOEC: 0.1 μM; Fig. 3A4) followed by a decrease at higher concentrations (≥ 10 μM). In both the MES23.5 and SH-SY5Y cells exposure to dinoseb resulted in a modest decrease in mitochondrial activity (LOEC: 100 μM; Fig. 3A4). Exposure to dinoseb resulted in a reduction of membrane integrity in

B

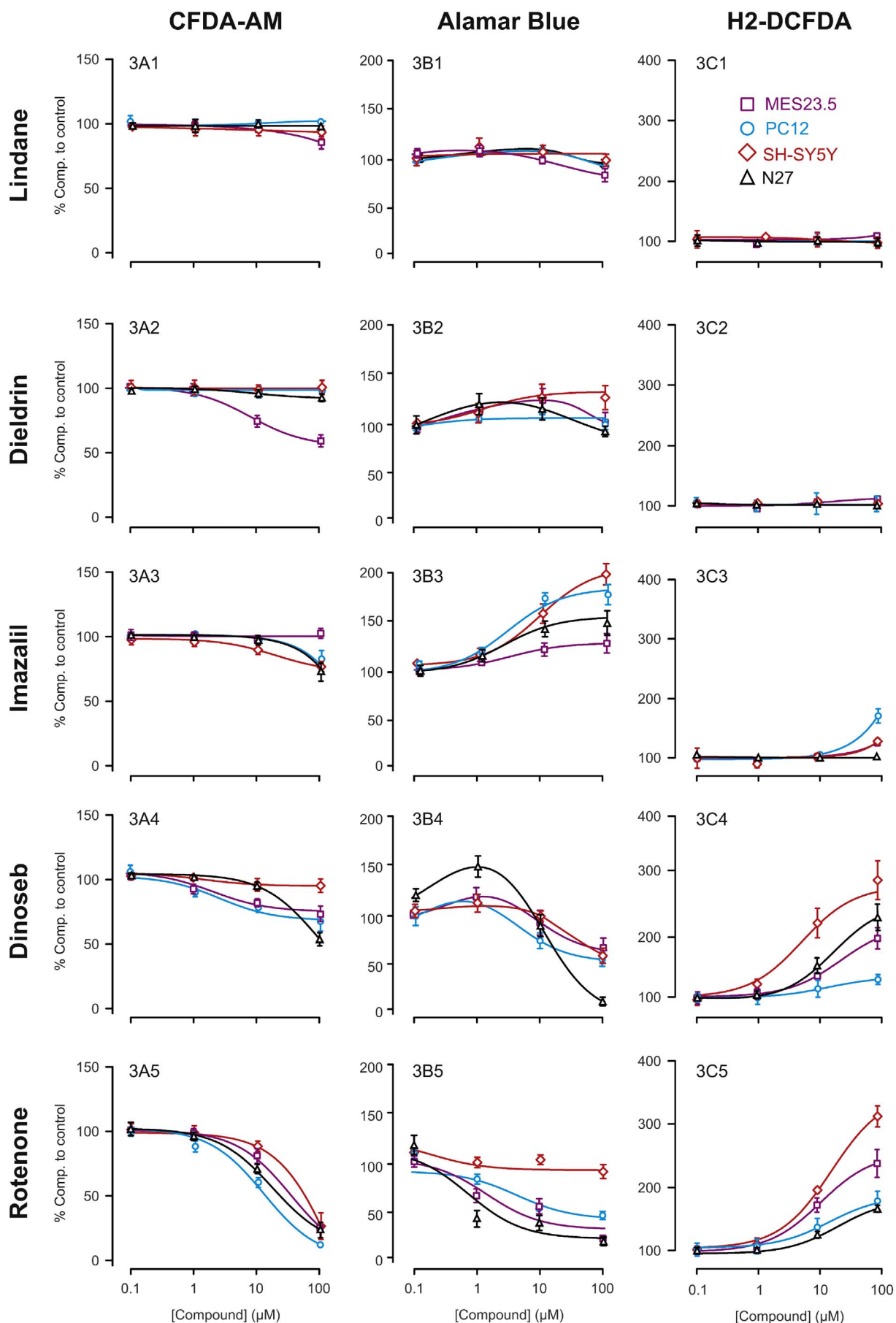| Cell line	Compound	Basal $[Ca^{2+}]_i$	K$^+$-evoked $[Ca^{2+}]_i$ (K2)
PC12	Lindane	↑ (S)	↓↓↓
	Dinoseb	↑ (T)	=
	Dieldrin	=	↓↓↓
	Rotenone	=	↓↓
	Imazalil	=	↓↓↓
SH-SY5Y	Lindane	=	↓↓
	Dinoseb	↑ (S)	↓↓
	Dieldrin	=	↓↓↓
	Rotenone	=	↓↓
	Imazalil	=	↓↓
MES23.5	Lindane	=	↓
	Dinoseb	↑ (T)	↑
	Dieldrin	=	↓↓↓
	Rotenone	=	↓↓
	Imazalil	=	↓↓↓
N27	Lindane	=	n.a.
	Dinoseb	↑ (T)	n.a.
	Dieldrin	=	n.a.
	Rotenone	=	n.a.
	Imazalil	=	n.a.

Fig. 2. Differential effects of pesticides on basal and depolarization-evoked $[Ca^{2+}]_i$. A Example traces of cytosolic $[Ca^{2+}]_i$ of individual PC12 cells, illustrating the inhibition of the second depolarization-evoked increase in $[Ca^{2+}]_i$ (K2) during exposure to DMSO (upper trace, control), 10 μM rotenone (middle trace) and 100 μM lindane (lower trace). The horizontal dashed lines indicate the duration of exposure. B Summary table of effects of the five reference pesticides (lindane 100 μM; dinoseb 30 μM; dieldrin 10 μM; rotenone 10 μM; imazalil 30 μM) on basal and depolarization-evoked $[Ca^{2+}]_i$ in the different cell lines. ↑ indicates an increase in $[Ca^{2+}]_i$ (≥ 25%), whereas ↓ indicates a decrease (↓: decrease ≤ 50%; ↓↓: decrease ≤ 75%; ↓↓↓: decrease > 75%), = indicates that no changes were observed. (T) indicates a transient increase in basal $[Ca^{2+}]_i$, whereas (S) indicates a sustained increase in $[Ca^{2+}]_i$. n.a.: not applicable.

(caption on next page)

Fig. 3. Differential effects of selected pesticides on membrane integrity (CFDA-AM, left column) and mitochondrial activity (alamar Blue, middle column) as measures of cell viability, as well as on ROS production (H_2DCFDA, right column) in PC12 (o), SH-SY5Y (◊), MES23.5 (☐) and N27 (Δ) cells following 24 h of exposure. The effects induced by particular pesticides differ between the various cell lines, resulting in different concentration-dependent changes in mitochondrial activity and membrane integrity. Data points in the concentration-response curves of the cell viability assays represent the average percentage membrane integrity (3A) or mitochondrial activity (3B) ($\pm$ SEM; ≥ 9 wells from ≥ 3 independent experiments) compared to control. The data points in the ROS production curves (3C) represent average percentage ROS production ($\pm$ SEM; ≥ 12 wells from ≥ 3 individual experiments) compared to time-matched control. (For interpretation of the references to colour in this figure legend, the reader is referred to the web version of this article.)

PC12, MES23.5 and N27 cells (LOECs 10, 10 and 100 μM respectively; Fig. 3B4), whereas no change in membrane integrity was observed in SH-SY5Y cells. Exposure to dinoseb induced ROS production in all cell lines (LOEC PC12: 100 μM; SH-SY5Y, MES23.5 and N27: 10 μM (Fig. 3C4). Comparable to the results observed with dinoseb, exposure to rotenone results in a bi-phasic concentration-response curve of mitochondrial activity in PC12 and N27 cells (both LOEC 0.1 μM; Fig. 3A5), whereas a concentration-dependent decrease is observed in MES23.5 and SH-SY5Y cells (both LOEC 1 μM; Fig. 3A5). In all cell lines, exposure to rotenone resulted in a decrease in membrane integrity (LOECs PC12: 1 μM; SH-SY5Y: 100 μM; MES23.5: 1 μM; N27: 1 μM; Fig. 3B5). Exposure to rotenone induced ROS production in all cell lines (LOEC rotenone 10 μM for all cell lines; Fig. 3C5).

4. Discussion

In this study we compared four catecholaminergic neuronal cell lines with respect to functional characteristics and toxicity of five known neurotoxic pesticides. The results presented in this paper clearly indicate that the observed effects of a compound depend on the cell line used and are thus likely related to intrinsic properties of the cell line, such as the expression of ion channels and receptors.

Calcium plays a pivotal role in many inter- and intraneuronal processes, including gene transcription (Carrasco and Hidalgo, 2006), neurotransmission (Westerink, 2006), neurodegeneration (Mattson, 2012) and neurodevelopment (Pravettoni et al., 2000). As such, changes in calcium homeostasis can be considered an important key event linking a molecular initiating event to a downstream adverse effect in so-called adverse outcome pathways (AOPs). Considering the different responses in $[Ca^{2+}]_i$ of the cell lines to the applied stimuli (Fig. 1), considerable differences in channel/receptor expression exist between the cell lines with MES23.5 cells being the most- and N27 cells the least versatile. The strong response of SH-SY5Y cells to ACh (100% response rate) indicates that SH-SY5Y cells can be used as a model for effects on ACh receptors. Although the approach used cannot be used to discriminate between ionotropic and metabotropic ACh receptors, data from literature suggests that both receptor types are present in undifferentiated SH-SY5Y cells (Vetter and Lewis, 2010). Therefore, the observed increase in $[Ca^{2+}]_i$ possibly consists of a combined influx from extracellular Ca^{2+} and store-mediated release of Ca^{2+}. In contrast, the SH-SY5Y cells did not respond to ATP indicating that these cells do not express P2X or P2Y purinergic receptors. This is in line with findings of Vetter and Lewis (Vetter and Lewis, 2010), but in contrast to earlier findings of Larsson and co-workers (Larsson et al., 2002) who reported the presence of P2X7 receptors in SH-SY5Y cells. This effectively illustrates that differences also may occur between clones of the same cell line, stressing the importance of knowing the properties of the cell line used when addressing compound-induced effects. As opposed to the non-responsive SH-SY5Y cell line, 32% of the N27 and 100% of the MES23.5 and PC12 cells in this study responded to ATP indicating the expression of functional purinergic receptors.

Furthermore, 74% of the MES23.5 cells responded to serotonin exposure indicative of the presence of 5-HT receptors, whereas the other cell lines did not show signs of functional 5-HT receptor.

Importantly, no response to glutamate was observed in either of the cell lines. While studies have been published in which these cell lines were exposed to high millimolar levels of glutamate to evoke cell death, the absence of glutamate-evoked calcium influx suggests it can be debated if this truly represents excitotoxicity. Consequently, the study of

this important pathway of neurotoxicity requires other (primary) cell models. The observation that PC12, MES23.5 and SH-SY5Y cells respond to high-K^+-induced depolarization and thus express VGCCs is in line with other research (Reuveny and Narahashi, 1991; Schneider et al., 1995; Shafer and Atchison, 1991). However, the types of VGCCs expressed differ among the cell lines as PC12 cells express L-, N- and P/Q-type VGCCs (Dingemans et al., 2009), whereas SH-SY5Y cells are reported to express L- and N-type VGCCs (Reuveny and Narahashi, 1991) and MES23.5 cells are reported to express predominantly N-type VGCCs (Schneider et al., 1995). As N27 cells do not respond to high-K^+-evoked depolarization, we conclude that N27 do not express functional VGCCs.

The differences in Ca^{2+} machinery between cell lines can lead to false-negative results when testing for neurotoxicity as illustrated by the observed absence of a lindane-induced effect on basal $[Ca^{2+}]_i$ in SHSY-5Y and MES23.5 cells. In PC12 cells, the increase in basal $[Ca^{2+}]_i$ upon exposure to lindane has been linked to a lindane-induced depolarization of the membrane of 32 mV (± 7 mV) causing opening of ω-conotoxin sensitive high-voltage activated calcium channels (N- and P/Q-type; Heusinkveld et al., 2010). This depolarization is apparently enough to reach the activation potential (V_a; Catterall et al., 2005) of the N- and P/Q-type VGCCs in PC12 cells, and to cause a Ca^{2+}-influx. As MES23.5 and SH-SY5Y are documented to express N-type VGCCs, but in particular the MES23.5 has a more negative membrane potential (see: Åkerman et al., 1984; Colom et al., 1998), the V_a is possibly not reached in these cells which may explain the absence of lindane-induced Ca^{2+} influx. Hence, the less negative membrane potential in PC12 cells renders these cells a good sentinel for neurotoxicity in excitable cells.

Furthermore, since the underlying mechanism of the dinoseb-induced increase in basal $[Ca^{2+}]_i$ is Ca^{2+} release from the endoplasmic reticulum (ER; Heusinkveld et al., 2016) the detection of dinoseb-induced increase in basal $[Ca^{2+}]_i$ in all cell lines is not surprising as all cells contain ER. However, the presence or absence of several channels and pumps as well as the coupling between ER and mitochondria may determine whether an increase in basal $[Ca^{2+}]_i$ is transient or sustained. Therefore, the observation that upon exposure to dinoseb a transient increase in $[Ca^{2+}]_i$ is observed in PC12, MES23.5 and N27 cells, whereas this transient increase is followed by a sustained increase in $[Ca^{2+}]_i$ in SH-SY5Y cells, is indicative for fundamental differences between the cell lines in Ca^{2+}-handling machinery. Also, the differences observed in the depolarization-induced increase in $[Ca^{2+}]_i$ upon exposure to dinoseb (MES23.5: increase; PC12: no effect) are likely explained by differences in intracellular Ca^{2+} handling and Ca^{2+}-related feedback loops. The observed dinoseb-induced decrease in depolarization-evoked $[Ca^{2+}]_i$ in human SH-SY5Y cells is most likely related to inhibition of VGCCs due to the sustained increase in $[Ca^{2+}]_i$. Altogether, this clearly demonstrates the importance of characterization of cell lines as the presence or absence of a toxic response can depend on rather subtle differences between cell lines.

Also the results from the experiments assessing the more general measures of toxicity (membrane integrity, mitochondrial activity and ROS production) demonstrate differences in sensitivity between cell lines. In general, the results clearly indicate that a change in mitochondrial activity is not necessarily linked to an increase in ROS production. Also, an increase in ROS production is not necessarily linked to more cell death. This is illustrated by the results from the human SH-SY5Y cell line that displays the highest relative ROS production in response to exposure to the mitochondrial toxicants dinoseb

and rotenone, whereas this cell line appears relatively insensitive in the membrane integrity and mitochondrial activity assays. This can likely be explained by differences in antioxidant levels and other coping strategies for oxidative stress between the cell lines. This is illustrated by the difference in results between imazalil and *e.g.* dinoseb as the imazalil-induced increase in mitochondrial activity only leads to a fairly mild ROS production in selected cell lines, whereas the changes in mitochondrial activity induced by dinoseb are paralleled by an increase in ROS production. Moreover, the hybrid cell line MES23.5 displays a particular, yet unexplained, sensitivity towards organochlorine insecticides as both exposure to lindane and dieldrin induced a change in membrane integrity solely in MES23.5 cells.

Thus, it appears that these cell lines differ considerably in their sensitivity towards toxicity for the different pesticides. It seems therefore justified to conclude that the research question should determine which model is the most appropriate since the intrinsic properties of a particular cell may strongly influence the outcome.

As exposure to all of these compounds is related to neurotoxicity related to changes in cellular function (intracellular Ca^{2+}), but not all are detected in general toxicity assays, measuring of cellular function appears pivotal to avoid false-negative results. Therefore, great care should be taken when interpreting toxicity data and the presented differences clearly highlight the need for thorough characterization of *in vitro* models. However, since the differential responses can be traced back to differences in membrane channel/receptor composition, using multiple cell lines may also provide mechanistic insight into the underlying mechanisms of action.

Transparency document

Acknowledgements/disclaimers

References

Adams, F.S., La Rosa, F.G., Kumar, S., Edwards-Prasad, J., Kentroti, S., Vernadakis, A., Freed, C.R., Prasad, K.N., 1996. Characterization and transplantation of two neuronal cell lines with dopaminergic properties. Neurochem. Res. 21, 619–627. http://dx.doi.org/10.1007/BF02527762.

Åkerman, K.E.O., Scott, I.G., Andersson, L.C., 1984. Functional differentiation of a human ganglion cell derived neuroblastoma cell line SH-SY5Y induced by a phorbol ester (TPA). Neurochem. Int. 6, 77–80. http://dx.doi.org/10.1016/0197-0186(84)90029-9.

Anand, M., Agrawal, A.K., Rehmani, B.N., Gupta, G.S., Rana, M.D., Seth, P.K., 1998. Role of GABA receptor complex in low dose lindane (HCH) induced neurotoxicity: neurobehavioural, neurochemical and electrophysiological studies. Drug Chem. Toxicol. 21, 35. http://dx.doi.org/10.3109/01480549809017849.

Biedler, J.L., Helson, L., Spengler, B.A., 1973. Morphology and growth, tumorigenicity, and cytogenetics of human neuroblastoma cells in continuous culture. Cancer Res. 33, 2643–2652. http://dx.doi.org/10.1007/PL00000826.

Bopp, S.K., Lettieri, T., 2008. Comparison of four different colorimetric and fluorometric cytotoxicity assays in a zebrafish liver cell line. BMC Pharmacol. 8, 8. http://dx.doi.org/10.1186/1471-2210-8-8.

Carrasco, M.A., Hidalgo, C., 2006. Calcium microdomains and gene expression in neurons and skeletal muscle cells. Cell Calcium 40 (575). http://dx.doi.org/10.1016/j.ceca.2006.08.021.

Catterall, W.A., Perez-Reyes, E., Snutch, T.P., Striessnig, J., 2005. International union of pharmacology. XLVIII. Nomenclature and structure-function relationships of voltage-gated calcium channels. Pharmacol. Rev. 57, 411. http://dx.doi.org/10.1124/pr.55.4.8.

Chen, L., Huang, E., Wang, H., Qiu, P., Liu, C., 2013. RNA interference targeting α-synuclein attenuates methamphetamine-induced neurotoxicity in SH-SY5Y cells. Brain Res. 1521, 59–67. http://dx.doi.org/10.1016/j.brainres.2013.05.016.

Colom, L.V., Diaz, M.E., Beers, D.R., Neely, A., Xie, W., Appel, S.H., 1998. Role of potassium channels in amyloid-induced cell death. J. Neurochem. 70, 1925–1934. http://dx.doi.org/10.1046/j.1471-4159.1998.70051925.x.

Corrigan, F.M., Wienburg, C.L., Shore, R.F., Daniel, S.E., Mann, D., 2000. Organochlorine insecticides in substantia nigra in Parkinson's disease. J. Toxicol. Environ. Health A 59, 229–234. http://dx.doi.org/10.1080/009841000156907.

Crawford, G.D., Le, W.D., Smith, R.G., Xie, W.J., Stefani, E., Appel, S.H., 1992. A novel N18TG2 × mesencephalon cell hybrid expresses properties that suggest a dopaminergic cell line of substantia nigra origin. J. Neurosci. 12, 3392–3398.

Dawson, T.M., Dawson, V.L., 2003. Molecular pathways of neurodegeneration in Parkinson's disease. Science 302, 819–823. http://dx.doi.org/10.1126/science.1087753.

Dingemans, M.M.L., Heusinkveld, H.J., De Groot, A., Bergman, Å., Van den Berg, M., Westerink, R.H.S., 2009. Hexabromocyclododecane inhibits depolarization-induced increase in intracellular calcium levels and neurotransmitter release in PC12 cells. Toxicol. Sci. 107, 490–497. http://dx.doi.org/10.1093/toxsci/kfn249.

Faria, J., Barbosa, J., Queirós, O., Moreira, R., Carvalho, F., Dinis-Oliveira, R.J., 2016. Comparative study of the neurotoxicological effects of tramadol and tapentadol in SH-SY5Y cells. Toxicology 359, 1–10. http://dx.doi.org/10.1016/j.tox.2016.06.010.

Franco, R., Li, S., Rodriguez-Rocha, H., Burns, M., Panayiotidis, M.I., 2010. Molecular mechanisms of pesticide-induced neurotoxicity: relevance to Parkinson's disease. Chem. Biol. Interact. 188 (289), 289–300. http://dx.doi.org/10.1016/j.cbi.2010.06.003.

Gleeson, E.C., Graham, J.E., Spiller, S., Vetter, I., Lewis, R.J., Duggan, P.J., Tuck, K.L., 2015. Inhibition of N-type calcium channels by fluorophenoxyanilide derivatives. Mar. Drugs 13, 2030–2045. http://dx.doi.org/10.3390/md13042030.

Gleichmann, M., Mattson, M.P., 2011. Neuronal calcium homeostasis and dysregulation. Antioxid. Redox Signal. 14, 1261–1273. http://dx.doi.org/10.1089/ars.2010.3386.

Goodwin, J., Nath, S., Engelborghs, Y., Pountney, D.L., 2013. Raised calcium and oxidative stress cooperatively promote alpha-synuclein aggregate formation. Neurochem. Int. 62, 703–711. http://dx.doi.org/10.1016/j.neuint.2012.11.004.

Greenamyre, J.T., Cannon, J.R., Drolet, R., Mastroberardino, P.-G., 2010. Lessons from the rotenone model of Parkinson's disease. Trends Pharmacol. Sci. 31 (141). http://dx.doi.org/10.1016/j.tips.2009.12.006.

Greene, L.A., Tischler, A.S., 1976. Establishment of a noradrenergic clonal line of rat adrenal pheochromocytoma cells which respond to nerve growth factor. Proc. Natl. Acad. Sci. U. S. A. 73, 2424. http://dx.doi.org/10.1073/pnas.73.7.2424.

Heusinkveld, H.J., Westerink, R.H.S., 2012. Organochlorine insecticides lindane and dieldrin and their binary mixture disturb calcium homeostasis in dopaminergic PC12 cells. Environ. Sci. Technol. 46, 1842–1848. http://dx.doi.org/10.1021/es203303r.

Heusinkveld, H.J., Thomas, G.O., Lamot, I., van den Berg, M., Kroese, A.B.A., Westerink, R.H.S., 2010. Dual actions of lindane (γ-hexachlorocyclohexane) on calcium homeostasis and exocytosis in rat PC12 cells. Toxicol. Appl. Pharmacol. 248, 12–19. http://dx.doi.org/10.1016/j.taap.2010.06.013.

Heusinkveld, H.J., Molendijk, J., Van den Berg, M., Westerink, R.H.S., 2013. Azole fungicides disturb intracellular Ca^{2+} in an additive manner in dopaminergic PC12 cells. Toxicol. Sci. 134, 374–381. http://dx.doi.org/10.1093/toxsci/kft119.

Heusinkveld, H.J., van Vliet, A.C., Nijssen, P.C.G., Westerink, R.H.S., 2016. In vitro neurotoxic hazard characterisation of dinitrophenolic herbicides. Toxicol. Lett. 252, 62–69. http://dx.doi.org/10.1016/j.toxlet.2016.04.014.

Larsson, K.P., Hansen, A.J., Dissing, S., 2002. The human SH-SY5Y neuroblastoma cell-line expresses a functional P2X7 purinoceptor that modulates voltage-dependent Ca^{2+} channel function. J. Neurochem. 83, 285–298. http://dx.doi.org/10.1046/j.1471-4159.2002.01110.x.

Lerner, I., Trus, M., Cohen, R., Yizhar, O., Nussinovitch, I., Atlas, D., 2006. Ion interaction at the pore of Lc-type Ca^{2+} channel is sufficient to mediate depolarization-induced exocytosis. J. Neurochem. 97, 116–127. http://dx.doi.org/10.1111/j.1471-4159.2006.03709.x.

Mattson, M.P., 2012. Parkinson's disease: don't mess with calcium. J. Clin. Invest. 122, 1195–1198. http://dx.doi.org/10.1172/JCI62835.

Meijer, M., Dingemans, M.M., van den Berg, M., Westerink, R.H., 2014. Inhibition of voltage-gated calcium channels as common mode of action for (mixtures of) distinct classes of insecticides. Toxicol. Sci. 141, 103–111. http://dx.doi.org/10.1093/toxsci/kfu110.

Palmeira, C.M., Moreno, A.J., Madeira, V.M.C., 1994. Interactions of herbicides 2,4-D and Dinoseb with liver mitochondrial bioenergetics. Toxicol. Appl. Pharmacol. 127 (50), 50–57. http://dx.doi.org/10.1006/taap.1994.1138.

Prasad, K.N., Carvalho, E., Kentroti, S., Edwards-Prasad, J., Freed, C., Vernadakis, A., 1994. Establishment and characterization of immortalized clonal cell lines from fetal rat mesencephalic tissue. In Vitro Cell. Dev. Biol. Anim. 30 A (596), 321–328.

Pravettoni, E., Bacci, A., Coco, S., Forbicini, P., Matteoli, M., Verderio, C., 2000. Different localizations and functions of L-type and N-type calcium channels during development of hippocampal neurons. Dev. Biol. 227, 581–594. http://dx.doi.org/10.1006/dbio.2000.9872.

Reuveny, E., Narahashi, T., 1991. Potent blocking action of lead on voltage-activated calcium channels in human neuroblastoma cells SH-SY5Y. Brain Res. 545 (312), 312–314. http://dx.doi.org/10.1016/0006-8993(91)91304-J.

Reuveny, E., Narahashi, T., 1993. Two types of high voltage-activated calcium channels in SH-SY5Y human neuroblastoma cells. Brain Res. 603, 64–73. http://dx.doi.org/10.1016/0006-8993(93)91300-H.

Sala, G., Marinig, D., Riva, C., Arosio, A., Stefanoni, G., Brighina, L., Formenti, M., Alberghina, L., Colangelo, A.M., Ferrarese, C., 2016. Rotenone down-regulates HSPA8/hsc70 chaperone protein in vitro: a new possible toxic mechanism contributing to Parkinson's disease. Neurotoxicology 54, 161–169. http://dx.doi.org/10.1016/j.neuro.2016.04.018.

Schneider, T., Perez-Reyes, E., Nyormoi, O., Wei, X., Crawford, G.D., Smith, R.G., Appel,

S.H., Birnbaumer, L., 1995. Alpha-1 subunits of voltage gated Ca²⁺ channels in the mesencephalon × neuroblastoma hybrid cell line MES23.5. Neuroscience 68, 479–485. http://dx.doi.org/10.1016/0306-4522(95)00147-B.

Shafer, T.J., Atchison, W.D., 1991. Transmitter, ion channel and receptor properties of pheochromocytoma (PC12) cells: a model for neurotoxicological studies. Neurotoxicology 12, 473.

Song, C., Kanthasamy, A., Jin, H., Anantharam, V., Kanthasamy, A.G., 2011. Paraquat induces epigenetic changes by promoting histone acetylation in cell culture models of dopaminergic degeneration. Neurotoxicology 32, 586–595. http://dx.doi.org/10.1016/j.neuro.2011.05.018.

Sousa, S.R., Vetter, I., Ragnarsson, L., Lewis, R.J., 2013. Expression and pharmacology of endogenous Cav channels in SH-SY5Y human neuroblastoma cells. PLoS One 8, e59293. http://dx.doi.org/10.1371/journal.pone.0059293.

Tanaka, T., 1995. Reproductive and neurobehavioral effects of imazalil administered to mice. Reprod. Toxicol. 9, 281–288. http://dx.doi.org/10.1016/0890-6238(95)00010-8.

Tully, K., Treistman, S.N., 2004. Distinct intracellular calcium profiles following influx through N- versus L-type calcium channels: role of Ca²⁺-induced Ca²⁺ release. J. Neurophysiol. http://dx.doi.org/10.1152/jn.01004.2003.

Vale, C., Fonfra, E., Bujons, J., Messeguer, A., Rodriguez-Farré, E., Sunol, C., 2003. The organochlorine pesticides gamma-hexachlorocyclohexane (lindane), alpha-endosulfan and dieldrin differentially interact with GABAₐ and glycine-gated chloride channels in primary cultures of cerebellar granule cells. Neuroscience 117, 397–403. http://dx.doi.org/10.1016/S0306-4522(02)00875-8.

Vaughan, P.F.T., Peers, C., Walker, J.H., 1995. The use of the human neuroblastoma SH-SY5Y to study the effect of second messengers on noradrenaline release. Gen. Pharmacol. 26, 1191–1201. http://dx.doi.org/10.1016/0306-3623(94)00312-B.

Vetter, I., Lewis, R.J., 2010. Characterization of endogenous calcium responses in neuronal cell lines. Biochem. Pharmacol. 79, 908–920. http://dx.doi.org/10.1016/j.bcp.2009.10.020.

Westerink, R.H., 2006. Targeting exocytosis: ins and outs of the modulation of quantal dopamine release. CNS Neurol. Disord. Drug Targets 5, 57–77. http://dx.doi.org/10.2174/18715270678411159.

Westerink, R.H., 2013. Do we really want to REACH out to in vitro? Neurotoxicology 39, 169–172. http://dx.doi.org/10.1016/j.neuro.2013.10.001.

Westerink, R.H.S., Ewing, A.G., 2008. The PC12 cell as model for neurosecretion. Acta Physiol. 192, 273. http://dx.doi.org/10.1111/j.1748-1716.2007.01805.x.

Xu, Q., Kanthasamy, A.G., Jin, H., Reddy, M.B., 2016. Hepcidin plays a key role in 6-OHDA induced iron overload and apoptotic cell death in a cell culture model of Parkinson's disease. Park. Dis. 2016, 8684130. http://dx.doi.org/10.1155/2016/8684130.

Zhao, H., Li, L., Fan, H.-J., Wang, F., Jiang, L.-M., He, P.-G., Fang, Y.-Z., 2012. Exocytosis of SH-SY5Y single cell with different shapes cultured on ITO micro-pore electrode. Mol. Cell. Biochem. 363, 309–313. http://dx.doi.org/10.1007/s11010-011-1183-9.

Zhu, D., Zhang, J., Wu, J., Li, G., Yao, W., Hao, J., Sun, J., 2016. Paliperidone protects SH-SY5Y cells against MK-801-induced neuronal damage through inhibition of Ca²⁺ influx and regulation of SIRT1/miR-134 signal pathway. Mol. Neurobiol. 53, 2498–2509. http://dx.doi.org/10.1007/s12035-015-9217-z.